

This document is confidential and is proprietary to the American Chemical Society and its authors. Do not copy or disclose without written permission. If you have received this item in error, notify the sender and delete all copies.

**Multifunctional nanovesicle-bioactive conjugates prepared
by a one-step scalable method using CO₂-expanded
solvents**

Journal:	<i>Nano Letters</i>
Manuscript ID:	Draft
Manuscript Type:	Communication
Date Submitted by the Author:	n/a
Complete List of Authors:	<p>Ventosa, Nora; Consejo Superior de Investigaciones Científicas (CSIC), Institut de Ciència de Materials de Barcelona (ICMAB) Cabrera, Ingrid; Consejo Superior de Investigaciones Científicas (CSIC), Institut de Ciència de Materials de Barcelona (ICMAB) Elizondo, Elisa; Consejo Superior de Investigaciones Científicas (CSIC), Institut de Ciència de Materials de Barcelona (ICMAB) Esteban, Olga; Institut de Bioenginyeria de Catalunya (IBEC), Corchero, José; CIBER de Bioingeniería, Biomateriales y Nanomedicina (CIBER-BBN), Institute for Biotechnology and Biomedicine, Universitat Autònoma de Barcelona Mergarejo, Marta; Combinatorial Chemistry Unit, Pulido, Daniel; Combinatorial Chemistry Unit, Cordoba, Alba; Consejo Superior de Investigaciones Científicas (CSIC), Institut de Ciència de Materials de Barcelona (ICMAB) Moreno-Calvo, Evelyn; Universitat de Barcelona, Cristal·lografia Mineralogia i Dipòsits Minerals Unzueta, Ugutz; fDepartament de Genètica i de Microbiologia, Vazquez, Esther; CIBER de Bioingeniería, Biomateriales y Nanomedicina (CIBER-BBN), Institute for Biotechnology and Biomedicine, Universitat Autònoma de Barcelona Abasolo, Ibane; Vall d'Hebron Institut de Recerca (VHIR), CIBBIM-Nanomedicine Schwartz, Simo; Vall d'Hebron Institut de Recerca (VHIR), CIBBIM-Nanomedicine Villaverde, Antonio; UAB, Albericio, Fernando; Institute for Research in Biomedicine-Barcelona, Barcelona Science Park Royo, Miriam; Combinatorial Chemistry Unit, Garcia-Parajo, Maria; Institute of Photonic Sciences, ICFO, Single Molecule Biophotonics Veciana, Jaume; Universitat de Bellaterra, Institut de Ciència Materials de Barcelona (CSIC)</p>

SCHOLARONE™
Manuscripts

1
2
3
4
5
6
7
8
9
10
11
12
13
14
15
16
17
18
19
20
21
22
23
24
25
26
27
28
29
30
31
32
33
34
35
36
37
38
39
40
41
42
43
44
45
46
47
48
49
50
51
52
53
54
55
56
57
58
59
60

1
2
3
4
5
6
7
8
9
10
11
12
13
14
15
16
17
18
19
20
21
22
23
24
25
26
27
28
29
30
31
32
33
34
35
36
37
38
39
40
41
42
43
44
45
46
47
48
49
50
51
52
53
54
55
56
57
58
59
60

Multifunctional nanovesicle-bioactive conjugates prepared by a one-step scalable method using CO₂- expanded solvents

*Ingrid Cabrera^{a,b}, Elisa Elizondo^{a,b}, Olga Esteban^{b,c}, Jose Luis Corchero^{b,d}, Marta Melgarejo^{b,e},
Daniel Pulido^{b,e}, Alba Córdoba^{b,a}, Evelyn Moreno^{a,b}, UgutzUnzueta^{b,d,f}, Esther Vazquez^{b,d},
IbaneAbasolo^{b,g}, Simó Schwartz Jr.^{b,g}, Antonio Villaverde^{b,f}, Fernando Albericio^{b,h,i,j}, Miriam
Royo^{e,b}, Maria F. García-Parajo^{k,l}, Nora Ventosa^{a,b,*}, JaumeVeciana^{a,b,*}*

^aInstitut de Ciència de Materials de Barcelona (ICMAB-CSIC), Campus Universitari de
Bellaterra, 08193 Cerdanyola del Vallès, Spain

^bCentro de Investigación Biomédica en Red –Bioingeniería, Biomateriales y Nanomedicina
(CIBER-BBN)

^cIntitut de Bioenginyeria de Catalunya (IBEC), BaldiriReixac 15-21, 08028 Barcelona, Spain

^dInstitut de Biotecnologia i de Biomedicina, Universitat Autònoma de Barcelona, 08193
Bellaterra, Spain

^eCombinatorial Chemistry Unit, Barcelona Science Park, BaldiriReixac 10, 08028 Barcelona,
Spain

^fDepartament de Genètica i de Microbiologia, Universitat Autònoma de Barcelona, 08193
Bellaterra, Spain

^gCIBBIM-Nanomedicine. VHIR Vall d'Hebron Institut de Recerca, 08035 Barcelona, Spain

^hInstitute for Reserch in Biomedicine (IRB Barcelona), 08028 Barcelona, Spain

ⁱDepartment of Organic Chemistry, University of Barcelona, MartíFranqués 1-11, 08028
Barcelona, Spain

^jSchool of Chemistry, University of KwaZulu-Natal, 4001-Durban, South Africa

^kICFO- Institut de Ciències Fotoniques, Mediterranean Technology Park, 08860 Castelldefels,
Barcelona, Spain

^lICREA-Institució Catalana de Recerca i Estudis Avançats, 08010 Barcelona, Spain

ABSTRACT. Integration of therapeutic biomolecules, such as proteins and peptides, in nanovesicles is a widely used strategy to improve their stability and efficacy. However, translation of these promising nanotherapeutics to clinical tests is still challenged by the complexity involved in the preparation of functional nanovesicles, their reproducibility, scalability and cost production. Here we introduce a simple one-step methodology based on the use of CO₂-expanded solvents to prepare multifunctional nanovesicle-bioactive conjugates. We demonstrate high vesicle-to-vesicle homogeneity in terms of size and lamellarity, batch-to-batch consistency and reproducibility upon scaling-up. Importantly, the procedure is readily amenable to the integration/encapsulation of multiple components into the nanovesicles in a single step and yields sufficient quantities for clinical research. The simplicity, reproducibility and scalability render this one-step fabrication process ideal for the rapid and low cost translation of nanomedicine candidates from the bench to the clinic.

KEYWORDS: Compressed fluids, bioconjugates, nanovesicles, liposomes, nanomedicine, scale-up

1
2
3
4
5
6
7
8
9
10
11
12
13
14
15
16
17
18
19
20
21
22
23
24
25
26
27
28
29
30
31
32
33
34
35
36
37
38
39
40
41
42
43
44
45
46
47
48
49
50
51
52
53
54
55
56
57
58
59
60

Liposomes, and in general vesicles, are undoubtedly one of the most promising supramolecular assemblies for nanomedicine due to their great versatility respect to size, composition, surface characteristics and capacity for integrating and encapsulating bioactive molecules. Their membranes can be efficiently functionalized with different targeting units like peptides, antibodies, etc., that promote specific and increased accumulation of the drug or the bioactive molecule in the target cells. Besides, they are well recognized as pharmaceutical carriers because of their biocompatibility, biodegradability and low toxicity.^{1,2} This has prompted their use in the treatment of some major health threats including cancer, infections, metabolic and autoimmune diseases, and has even led to first marketed products.^{3,4} Important pharmacological specifications like stability, loading capability, leakage kinetics of entrapped substances, etc, are determined by the structural characteristics (e.g. size, morphology, supramolecular organization, structural homogeneity) of these nanocarriers.⁵ For instance small unilamellar vesicles (SUVs) with sizes around 100 nm, have attracted great attention in the drug delivery field. These vesicles are large enough to avoid the first-pass elimination through the kidneys but sufficiently small to present a minimal uptake by the mononuclear phagocytic system, facilitating their longer circulation lifetime in the body and hence higher possibility to reach the target cells. Moreover, due to their nano-scale size SUVs can accumulate within tumours through the enhanced permeability and retention (EPR) effect and thereby be applied in cancer therapy.⁶ Methods to produce SUVs commonly use conventional techniques for vesicle formation such as lipid thin-film hydration^{7,8} or reverse-phase evaporation,^{9,10} and further post-formation steps (sonication,^{11,12} extrusion,^{13,14} etc) for size reduction and homogenization. These conventional processes are generally complex, multi-step, time consuming, not easily scalable and might damage the functionality of the bioactive molecules. All these drawbacks are particularly relevant in the preparation of colloidal

1
2
3 bioconjugates with expensive and/or fragile active biomolecules, such as proteins, peptides,
4 enzymes, hormones, etc. Thus, it is crucial the development of simple and mild processes that
5 allow the control of the structure at the micro-, nano- and supramolecular levels and are
6 amenable to be scalable.¹⁵
7
8
9

10
11
12 Compressed fluid-based methodologies, also named as dense gas technologies, are attracting
13 increasing interest for the direct preparation of micro/nanoparticulate materials with structural
14 characteristics not reachable by already existing particle production procedures using liquid
15 solvents.^{16,17} Compressed fluids are defined as substances that at normal conditions of pressure
16 and temperature exist as gases but increasing the pressure can be converted into liquids or
17 supercritical fluids, and be used as solventmedia for chemical and material processing.^{18,19}
18
19
20
21
22
23
24
25
26

27 Recently, we have developed a procedure called DELOS-SUSP (Depressurization of an
28 Expanded Liquid Organic Solution-Suspension) for the preparation of dispersed systems. Using
29 this methodology the straightforward synthesis of cholesterol-rich SUVs with controlled size
30 distributions, uniform shapes and good stability in time, has been achieved.²⁰ In addition, recent
31 studies have shown that vesicular systems prepared by this method have a vesicle-to-vesicle
32 homogeneity degree, regarding membrane supramolecular organization, more than double than
33 those prepared by thin-film hydration.²¹
34
35
36
37
38
39
40
41
42

43 Here we demonstrate the potentiality of the DELOS-SUSP method as a simple, robust,
44 scalable and one-step process to prepare a variety of multifunctional SUV-biomolecule
45 conjugates with high structural homogeneity. In particular, we report the straightforward
46 functionalization of vesicle membranes with two different molecular units: 1) the hydrophilic
47 poly(ethylene glycol) (PEG) polymer, a stealth agent widely used to prolong circulation time by
48 stabilizing and protecting the vesicles against phagocytosis, and 2) a targeting RGD cyclic
49
50
51
52
53
54
55
56
57
58
59
60

1
2
3 peptide known to increase the cell penetration via RGD/integrin recognition. We also present the
4 one-step integration of two hydrophilic model proteins: 1) the green fluorescence protein (GFP)
5 and 2) the bovine serum albumin (BSA) as well as the preparation of multifunctional vesicles
6 integrating simultaneously two active molecules. As depicted in Figure1, nanovesicle-bioactive
7 conjugates were prepared using two different membrane chemical compositions. In one
8 formulation the membrane was formed by cholesterol and the phospholipid 1,2-dipalmitoyl-*sn*-
9 glycerol-3-phosphocholine (DPPC) yielding SUVs, from now on called Liposomes. The second
10 formulation, much less common and presenting a positively charged membrane, is composed by
11 cholesterol and hexadecyltrimethylammonium bromide (CTAB) surfactant, yielding SUVs
12 named as Quatsomes.²²

13
14
15 All bioconjugates were prepared several times following the procedure schematically represented
16 in Figure2, always under mild conditions to preserve the activity of labile biomolecules (See
17 Table 1 and Supporting Information Figure 1). Briefly, the method consists in loading a solution
18 of the membrane lipid components and the desired hydrophobic bioactives in an organic solvent
19 (e.g. ethanol) into a high-pressure autoclave and pressurizing it with a large amount of
20 compressed CO₂. Vesicular nanoconjugates are formed, by depressurizing the resulting CO₂-
21 expanded solution over an aqueous phase, which might contain water soluble surfactants and
22 hydrophilic bioactives (Supporting Information). The experimental conditions used for the
23 preparation of the organic and aqueous phases of each formulation are given in Table 2. No
24 further energy input is required for achieving the desired SUVs structural characteristics, neither
25 for increasing the loading or functionalization efficiencies. The CO₂ here acts as a co-solvent and
26 its evaporation from the organic expanded solution during the depressurization stage produces a
27 fast, large and homogeneous cooling responsible of the high vesicle-to-vesicle structural
28
29
30
31
32
33
34
35
36
37
38
39
40
41
42
43
44
45
46
47
48
49
50
51
52
53
54
55
56
57
58
59
60

1
2
3 homogeneity in comparison to that reached by conventional thin-film hydration. It should be
4
5 pointed out, that lipids, such as cholesterol, have a great sensitivity to solvent media variations.²³
6
7
8 Therefore, homogeneous vesicle formation paths are required to guarantee a high degree of
9
10 structural homogeneity.
11

12 **Nanovesicle-PEG conjugates**

13
14
15 One of the most spread strategies to avoid the fast clearance of vesicles by opsonisation and to
16
17 increase the blood circulation periods in the body is the coating of the carrier membranes with
18
19 hydrophilic biocompatible polymers such as polyethyleneglycol polymers (PEGs).²⁴ These so-
20
21 called long-circulating or stealth liposomes experience a “passive” accumulation in tumours and
22
23 inflammations, enhancing the drug delivery in these affected parts.²⁵ Conventional
24
25 methodologies like lipid thin-film hydration or reverse-phase evaporation are generally
26
27 employed to prepare PEGylated liposomes using small concentrations (≤ 7 mol %) of short-chain
28
29 PEGs (1000-4000 Daltons) covalently linked to selected lipid membrane constituents. Nanosized
30
31 PEGylated Liposomes and PEGylated Quatsomes were straightforward produced by DELOS-
32
33 susp, adding cholesterol_PEG₁₀₀₀ and cholesterol_PEG₂₀₀₀ as part of the vesicle membrane
34
35 components (Figure 1). To prepare the Quatsome-PEG conjugates, a CO₂-expanded solution of
36
37 cholesterol and cholesterol_PEG (6:1 molar ratio) in ethanol was depressurized over an aqueous
38
39 solution containing CTAB. In the case of Liposome-PEG conjugates, the CO₂-expanded
40
41 alcoholic phase, composed by cholesterol, DPPC and cholesterol_PEG, was depressurized over
42
43 water. In all experiments the molar ratio between cholesterol and cholesterol_PEG was 6:1.
44
45 Cryo-transmission electron microscopy (Cryo-TEM) images of the resulting PEGylated SUVs,
46
47 disclosed homogeneous, spherically shaped and unilamellarnanovesicles in all cases (Figure 3a-
48
49 3d). Their size distribution, polydispersity index and Z potential were determined using dynamic
50
51
52
53
54
55
56
57
58
59
60

1
2
3 light scattering (DLS) and are reported in Table 1. The Quatsome-PEG conjugates presented
4 smaller particle sizes and polydispersity indices. Besides their absolute Z potential values were
5 larger than 30 mV consistent with a higher stability under storage conditions (Supporting
6 Information). Indeed, no changes in size and morphology were observed for more than one year,
7 indicating that these vesicular systems are very stable and do not suffer aggregation upon long
8 periods of time. This stability was somewhat smaller in the case of Liposome-PEG formulations
9 which presented Z potentials between 7 and 13 mV. Nevertheless, the suspensions were
10 macroscopically stable during at least 30 days, with no evidence of solid deposition. The high
11 stability of Quatsome-PEG conjugates is explained by the particular self-assembling of
12 cholesterol and CTAB molecules to form vesicular structures with outstanding stability.²²

26 27 **Nanovesicle-RGD conjugates**

28
29 “Active targeting” through the incorporation of specific molecules on the outer surface of
30 vesicles can provide more effective therapeutic action to a nanomedicine.¹ In the last years the
31 RGD-peptide has become the ligand of choice for the labelling of liposomes due to its capacity
32 of binding integrin receptors, over expressed in tumor cells.²⁶ Among the different types of RGD
33 peptides available we chose the cRGDfK to functionalize our Liposomes due to several
34 advantages related with its cyclic structure.²⁷ We synthesized a cholesterol_PEG₂₀₀_RGD
35 molecule, in which the cholesterol was first attached to a PEG₂₀₀ unit through an ether bond and
36 the cRGDfK peptide was coupled to this unit through a carbamate bond (Supporting
37 Information). For the one-step preparation of Liposome-RGD conjugates, a mixture of
38 cholesterol, DPPC and cholesterol_PEG₂₀₀_RGD in a molar ratio of 6:10:1 was dissolved in
39 ethanol and then expanded with CO₂. Once the depressurization over water took place, a
40 suspension of functionalized nanovesicles was obtained with a narrow particle size distribution
41
42
43
44
45
46
47
48
49
50
51
52
53
54
55
56
57
58
59
60

1
2
3 centered in 144 nm and macroscopically stable for at least 30 days (Table 1, Supporting
4 Information). Cryo-TEM images (Figure 3e) revealed a much more homogeneous unilamellar
5 system when cholesterol_PEG₂₀₀_RGD was inserted in the membrane compared to plain
6 liposomes, which was also confirmed with small-angle X-ray scattering (SAXS) measurements
7 (Supporting Information and Supporting Information Figures S3 and S5). Furthermore, an
8 increase in the Z potential from less than +10 mV up to +30 mV was observed when
9 cholesterol_PEG₂₀₀_RGD was present in the formulation (Table 1), leading to a higher stability
10 of the vesicular system along time. To enquire whether this higher structural homogeneity was
11 related to the use of the DELOS-SUSP method to produce the liposomes or exclusively due to
12 the presence of the peptide, we prepared the Liposomes containing cholesterol_PEG₂₀₀-RGD
13 using the conventional lipid thin-film hydration methodology (Supporting Information). The
14 resulting formulation was less homogeneous, highly unstable and multilamellar showing a size
15 distribution centered at 1926 nm (Supporting Information Figure S4). This demonstrates that
16 both, the presence of the cholesterol_PEG₂₀₀_RGD molecule as well as the preparation
17 methodology are key ingredients for the synthesis of these highly homogeneous conjugates. It is
18 worthy to say that while it took 2 hours to prepare 25 mL of this nanoconjugate suspension by
19 the CO₂-based procedure, 2 days were required for the preparation of 2mL of nanovesicles-RGD
20 by thin-film hydration plus post-formation steps.
21
22
23
24
25
26
27
28
29
30
31
32
33
34
35
36
37
38
39
40
41
42
43
44
45

46 To determine the amount of cholesterol_PEG₂₀₀_RGD incorporated into the membrane, the
47 fraction of non-integrated molecules was separated from the total sample using centrifugal filter
48 devices (Centricons) of 30 kDa and then analyzed by HPLC (Supporting Information). The
49 analysis showed the absence of free peptide in the mother liquors, resulting in almost a 100%
50 incorporation of the cholesterol functionalized with the peptide within the lipid bilayer. A similar
51
52
53
54
55
56
57
58
59
60

1
2
3 high degree of RGD incorporation was achieved by Schiffelers *et al.* using the conventional lipid
4 thin-film hydration methodology.²⁸ Thus the DELOS-SUSP methodology allows a one-step
5 production of unilamellar conjugates in smaller processing times, with minimum material loss
6 and high yields of the ligand in the final formulation.
7
8
9

10
11
12 To investigate whether the activity of the integrated biomolecule is maintained during the
13 processing with CO₂-expanded solvents, we examined the internalization capabilities of the new
14 Liposome-RGD conjugates on endothelial (HMEC-1) cells which express high levels of $\alpha_v\beta_3$
15 integrins on both their apical and basal membranes²⁹ (Supporting Information Figure S4). For
16 this study the 1,1'-dioctadecyl-3,3,3',3'-tetramethylindodicarbocyanine perchlorate (DiD)
17 fluorescent dye was integrated into the membranes of Liposomes and Liposome-RGD conjugates
18 at a concentration of 0.6 nM (Supporting Information Figures S7 and S8), taking advantage of its
19 lipophilicity. HMEC-1 cells were then incubated with DiD-labelled liposomes with and without
20 RGD, for 3 hours at 37°C, to induce internalization and were subsequently inspected by laser
21 scanning confocal microscopy (LSCM). Liposome-RGD conjugates were rapidly uptaken by the
22 cells (Figure 4a) whereas the control plain Liposomes were barely internalized (Figure 4b).
23
24 Importantly, a fraction of Liposome-RGD conjugates trafficked to endosomal/lysosomal
25 compartments as judged by colocalization studies with the DiD (red) fluorophore and the
26 LysoTracker (green), a fluorescent probe which labels and tracks acidic organelles in live cells.
27
28 Indeed, three-dimensional reconstructions of z-stacked fluorescence images of live HMEC-1
29 showed colocalization between DiD-labelled Liposome-RGD conjugates and LysoTracker after 3
30 h of incubation at 37°C (Figure 4c). These data strongly indicate that the presence of RGD
31 peptides on the liposomes membrane enhance their binding and uptake by HMEC-1 via $\alpha_v\beta_3$
32 integrin-mediated endocytosis. The results were further confirmed on a large population of cells
33
34
35
36
37
38
39
40
41
42
43
44
45
46
47
48
49
50
51
52
53
54
55
56
57
58
59
60

1
2
3 using flow cytometry analysis. Indeed, about 85% of the cells showed enhanced fluorescence
4 when incubated with DiD-labelled Liposome-RGD conjugates at 37°C, whereas this percentage
5 was reduced to 4% for cells incubated with DiD-labelled plain Liposomes (Figure 4d).
6
7 Furthermore, a decrease in the fraction of positive cells was observed when cells were pulsed
8 with DiD-labelled Liposome-RGD conjugates at 16°C, a temperature that reduces endocytosis
9 (Figure 4d). The mean fluorescence intensity (MFI) values measured for HMEC-1 incubated
10 with DiD-labelled Liposome-RGD conjugates were 30-fold higher than those of the cells
11 incubated with DiD-labelled Liposomes (Figure 4e), demonstrating that the presence of the
12 peptide is responsible for the enhanced liposome uptake levels. These studies also confirm that
13 the DELOS-SUSP methodology did not affect the bioactivity of the RGD peptide after its
14 processing with compressed CO₂. Further *in vitro* assays showed that these nanocarriers were
15 non-toxic, non-hemolytic ($\leq 2\%$) and sterile, rendering them as excellent candidates for the
16 specific delivery of active molecules to targeted cells (Supporting Information Figures S9 and
17 S10).³⁰

36 **Nanovesicle-protein conjugates**

37
38 Nowadays, therapeutic proteins are attracting the attention of clinicians for the treatment of
39 many diseases as they are well tolerated by the body and have the ability to perform specific
40 functions without interfering with normal biological processes.³¹ However, the inherent lability
41 associated with proteins, including thermal instability, degradation by proteolysis, rapid body
42 excretion and low solubility, hinder the rapid progression of this field. Some drug delivery
43 systems such as polymeric nanoparticles or liposomes have been used to overcome these
44 limitations.³² Indeed, there are several examples of enzymes and hormones, among other
45 biomolecules,^{33,34} encapsulated into vesicles, which show a considerable increase of their
46
47
48
49
50
51
52
53
54
55
56
57
58
59
60

1
2
3 therapeutic activities. These systems are generally obtained using methodologies that require
4 further post-formation steps to achieve the desired size and to reduce the multilamellarity, steps
5 that sometimes affect the final protein-to-lipid ratio and reduce the drug activity in the resulting
6 formulation.³⁵ To evaluate the performance of the DELOS-SUSP methodology for encapsulating
7 proteins ensuring that their biological activity is preserved, we integrated two different model
8 proteins into SUVs: a modified GFP protein, the GFP-H6 (~27 KDa) tagged with six histidine
9 residues (Supporting Information), and the commercially available BSA protein (66.5 KDa). We
10 chose GFP because is usually employed as a natural marker for gene expression^{36,37} and has been
11 incorporated into micelles,³⁸ polymeric particles³⁹ or protein capsids.⁴⁰ On the other hand BSA is
12 the most abundant protein in the blood and has been extensively used as a model protein in
13 studies such as protein-membrane association,⁴¹ protein-surfactants interaction⁴² and for
14 entrapping into liposomes.⁴³

15
16
17
18
19
20
21
22
23
24
25
26
27
28
29
30
31
32 The preparation of Liposome-GFP conjugates was performed by depressurizing a CO₂-
33 expanded ethanolic solution of DPPC and cholesterol over a Tris buffer saline solution
34 containing the GFP-H6 protein. DLS measurements showed a size distribution centered at 228
35 nm (Table 1) and Cryo-TEM images revealed a homogeneous morphology (Figure 3f). The Z
36 potential was low, near zero, but the formulation remained macroscopically stable for more than
37 one week. The fluorescence of the GFP-H6 protein after processing, along with the confirmation
38 of its entrapment in the liposomes was assessed using dual colour total internal reflection
39 fluorescence (TIRF)-Epi microscopy. For this purpose DiD was also chosen as a membrane
40 marker for labelling the protein-loaded liposomes at a concentration of 0.6 nM (Supporting
41 Information Figure S7). A sample of 200 µl of DiD-labeled Liposome-GFP conjugate was
42 deposited on a glass coverslip mounted into a microscope chamber. EPI-TIRF images were
43
44
45
46
47
48
49
50
51
52
53
54
55
56
57
58
59
60

1
2
3 collected in two different channels, red and green, to allow the simultaneous monitoring of the
4 signals from DiD and GFP, respectively. The spatial colocalization of both signals confirmed
5 that the GFP-H6 was successfully incorporated into liposomes and that its fluorescence was not
6 affected upon processing (Supporting Information Figure S11). To determine the amount of
7 protein incorporated, the free GFP-H6 was first separated from the loaded liposomes using
8 centrifugal filter devices of 100 KDa. The loaded vesicles were analyzed by SDS-PAGE and
9 further Western-blot (Supporting Methods) and the entrapment efficiency (%EE) was calculated
10 by dividing the mass of integrated active between the total initial mass. A 44 ± 7 % of protein
11 encapsulation within the liposomes was obtained for a 0.4 μmol protein/mmol total lipid in the
12 final formulation. This encapsulation efficiency value resulted fairly high considering that
13 hydrosoluble proteins generally presents low encapsulations efficiencies, especially in small
14 vesicles with diameters ranging from 50 to 150 nm.³⁵

15
16
17 To perform the entrapment of BSA (66.5 KDa) we chose Quatsomes, since these vesicular
18 structures are promising nanocarriers for the topical delivery of therapeutic biomolecules, like
19 enzymes, becoming a real alternative to phospholipid liposomes and non-ionic surfactant
20 niosomes.⁴⁴ Following the procedure schematized in Figure 2, an expanded organic solution
21 containing cholesterol was depressurized over an aqueous phase containing CTAB and the
22 protein. A macroscopically stable disperse system, with a very narrow size distribution centered
23 in 122 nm, was achieved (Table 1). The Z potential value was high and positive in agreement
24 with the membrane composition and the fact that the system remains stable over a period larger
25 than 5 months (Supporting Information). The Cryo-TEM images (Figure 3g) showed a
26 homogeneous system with nanoscopic, spherical and unilamellar vesicular structures. To
27 determine the encapsulation efficiency the BSA-loaded vesicles were separated from the non-

1
2
3 incorporated protein using centrifugal filter devices of 100 kDa. Free BSA in the supernatant was
4
5 quantified using a colorimetric method (Supporting Information). The entrapment efficiency in
6
7 the vesicles was calculated subtracting the mass of free protein to the initial mass and dividing
8
9 the result between the initial protein mass. A 96 ± 1.3 % of protein entrapment in the Quatsomes
10
11 was found which resulted in an extremely high value, considering that BSA is hydrosoluble and
12
13 that the vesicles are of nanoscopic size. A reasonable explanation for this high degree of
14
15 encapsulation is related to the presence of protein-membrane interactions. Indeed, BSA has a
16
17 negative charge under the entrapment conditions (isoelectric point of 4.7 in water), and therefore
18
19 could form a complex with the cationic nanovesicles. This complex together with the entrapment
20
21 of the protein inside the aqueous core of the vesicles explains the high encapsulation
22
23 efficiency. Thus, the use of DELOS-SUSP methodology for encapsulating BSA in Quatsomes
24
25 gave rise to high protein loadings, long stabilities in time and very homogeneous morphological
26
27 characteristics meliorating the association efficiencies achieved (20-75 %) for the encapsulation
28
29 of BSA in liposomes with conventional methodologies.⁴⁵ Additionally, this production platform
30
31 allows the preparation of nanovesicle-protein conjugates without damaging the activity of the
32
33 protein and with high final/raw protein ratios.

40
41 We also extended the DELOS-SUSP method to the simultaneous PEGylation and protein
42
43 loading of Quatsomes. A CO₂-expanded ethanolic solution containing cholesterol and
44
45 cholesterol_PEG₁₀₀₀ was depressurized over an aqueous solution containing CTAB and BSA at
46
47 same concentrations used in the previous experiments. Multifunctional conjugates with
48
49 nanoscopic size, homogeneous morphology and great stability in time were obtained together
50
51 with an 84 ± 3 % of BSA entrapment efficiency (Table 1, Figure 3h). These results show that the
52
53
54
55
56
57
58
59
60

1
2
3 reported methodology allows the preparation of multifunctional vesicles with high structural
4
5 homogeneity in terms of size and lamellarity, and high protein loadings.
6
7

8 **Scaling-up production of nanovesicle-bioactive conjugates**

9

10 Finally, bench-scale to clinical-scale reproducibility was check in order to evaluate the
11
12 potentiality of this new platform for the production of nanovesicle-bioactive conjugates with
13
14 sufficient quantities for clinical studies. The encapsulation of BSA in Quatsomes, as a model
15
16 formulation, was repeated under the same experimental conditions but in a 40 times larger high
17
18 pressure vessel (from 7.5 mL to 315 mL) using the same equipment configuration with minor
19
20 modifications in the automation procedure (Supporting Information Figure S2 and S12). With
21
22 this scale-up the batch volume of vesicle suspension was increased from milliliter up to liter
23
24 scale, which could allow the production of nanomedicine batches to be used in pre-clinical and
25
26 even clinical studies. The influence of DELOS-SUSP scale-up on the physicochemical
27
28 characteristics of the BSA-loaded Quatsomes was analyzed in terms of size, morphology and
29
30 entrapment efficiency. The resulting vesicles presented diameters around 123 nm with narrower
31
32 particle size distributions (Figure 5), indicating that even a more homogeneous system is
33
34 obtained at large scale. The differences in homogeneity are most probably due to the variance of
35
36 the configuration between the two equipments in the depressurization stage. Thus, in the case of
37
38 the large vessel, the manual depressurization valve was substituted for an automatic
39
40 depressurization valve that allows a better control and hence higher vesicle homogeneity and
41
42 batch-to-batch reproducibility. Cryo-TEM images depicted unilamellar and spherical
43
44 nanovesicles confirming the great degree of homogeneity achieved (Figure 5). According to
45
46 MicroBCA protein assay, 99 % of BSA was entrapped into the Quatsomes prepared with the
47
48 larger reactor, similar to the values obtained when using the smaller one. Moreover it is
49
50
51
52
53
54
55
56
57
58
59
60

1
2
3 important to highlight here that DELOS-SUSP operates under sterile conditions due to the use of
4 compressed CO₂, which is another important issue in the manufacturing of vesicles for human
5 and animal use.⁴⁶ The good reproducibility in terms of encapsulation percentages and
6 physicochemical characteristics between batches produced with the two reactors, demonstrate
7 the feasibility of scaling-up the method for the encapsulation of hydrosoluble proteins.
8
9

10
11 In conclusion, we have demonstrated that DELOS-SUSP methodology is a platform that
12 enables an easy and direct preparation of different SUV-biomolecule conjugates with nanoscopic
13 size and great degree of unilamellarity. Moreover, this platform shows “batch-to-batch”
14 consistency and allows the preparation of sufficient quantities of nanotherapeutics for clinical
15 testing. This one-step process allows the preparation of nanovesicles loaded with hydrosoluble
16 proteins, vesicular conjugates functionalized with targeting peptides or stealth polymers with
17 excellent perspectives as drug delivery platforms, and if desired/needed the incorporation of two
18 biomolecules simultaneously. Bioactivity of the integrated molecules is unaffected under the
19 processing conditions with CO₂-expanded solvents. The method overcomes major limitations
20 related with conventional methodologies and offers the possibility to synthesize a great variety of
21 nanovesicle based formulations, in a simpler, less time consuming and more environmentally
22 friendly way. Finally this method may be easily scaled-up following the Good Manufacturing
23 Practices requirements, becoming an attractive methodology for accelerating the clinical
24 translation of nanomedicines based on nanovesicles.
25
26
27
28
29
30
31
32
33
34
35
36
37
38
39
40
41
42
43
44
45
46
47
48
49
50
51
52
53
54
55
56
57
58
59
60

FIGURES

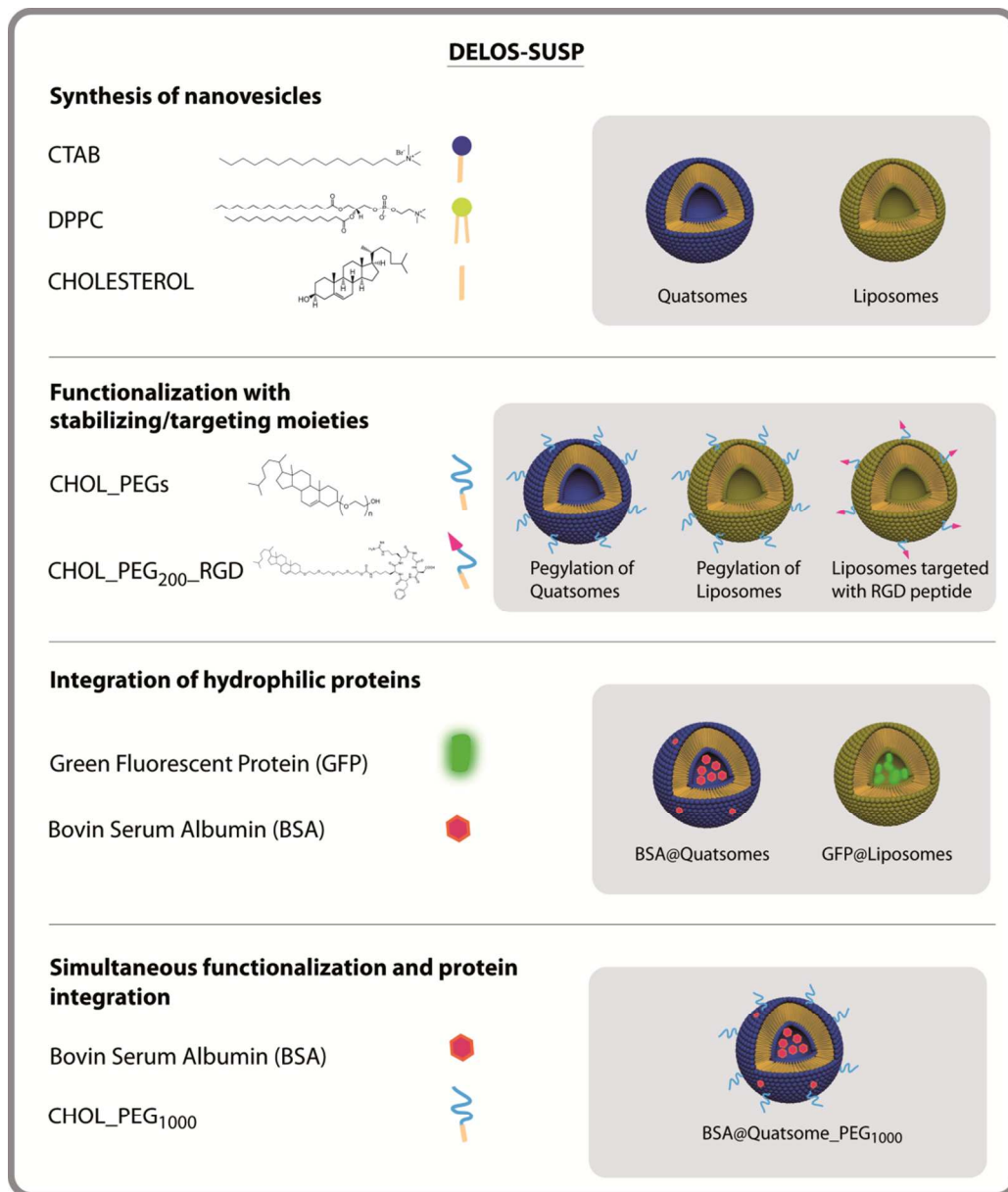


Figure 1. Schematic representation of multifunctional nanovesicle-bioactive conjugates prepared by DELOS-SUSP method and the molecular structure of their components.

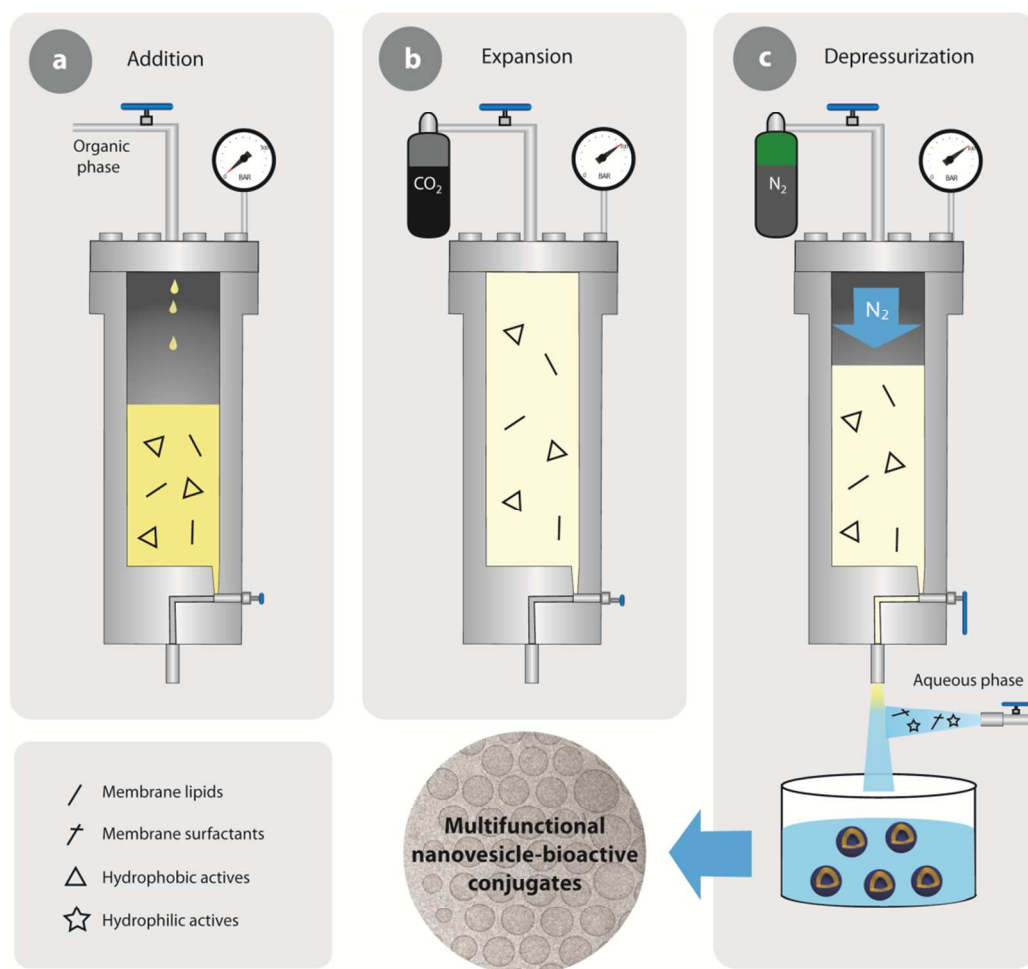


Figure 2. Schematic representation of the DELOS-SUSP method for efficient preparation of multifunctional nanovesicle-bioactive conjugates. The whole procedure includes the loading (a) of an organic solution of the lipidic membrane components and the desired hydrophobic active compounds/molecules into an autoclave at a working temperature (T_w) and atmospheric pressure. The addition of CO₂ (b) to produce a CO₂-expanded solution, at a given X_{CO_2} , working pressure (P_w) and T_w , where the hydrophobic actives and membrane components remain dissolved. Finally, the depressurization (c) of the expanded solution over an aqueous solution, which might contain membrane surfactants and hydrophilic biomolecules, to produce an aqueous dispersion

of the nanovesicle-bioactive(s) conjugates with vesicle-to-vesicle homogeneity regarding size and morphology.

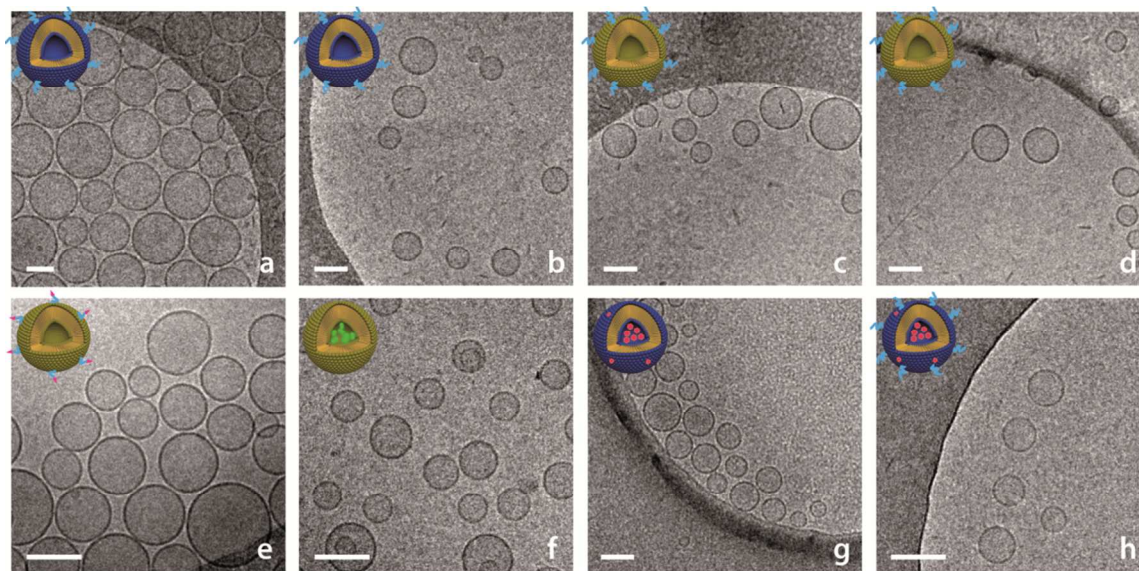


Figure 3. Cryo-Transmission Electron Microscopy images of nanovesicle-bioactive conjugates produce by DELOS-SUSP. a, PEGgylatedQuatsomes with cholesterol_PEG1000. b, PEGgylatedQuatsomes with cholesterol_PEG2000. c, PEGylated Liposomes with cholesterol_PEG1000. d, PEGylated Liposomes with cholesterol_PEG2000. e, Functionalized Liposomes with targeting units of cholesterol_PEG200_RGD. f, Liposomes with integrated GFP protein. g, Quatsomes with integrated BSA protein. h, Quatsomes functionalized with a stabilizing cholesterol_PEG1000 unit and integrated BSA protein. Scale bars are 100 nm.

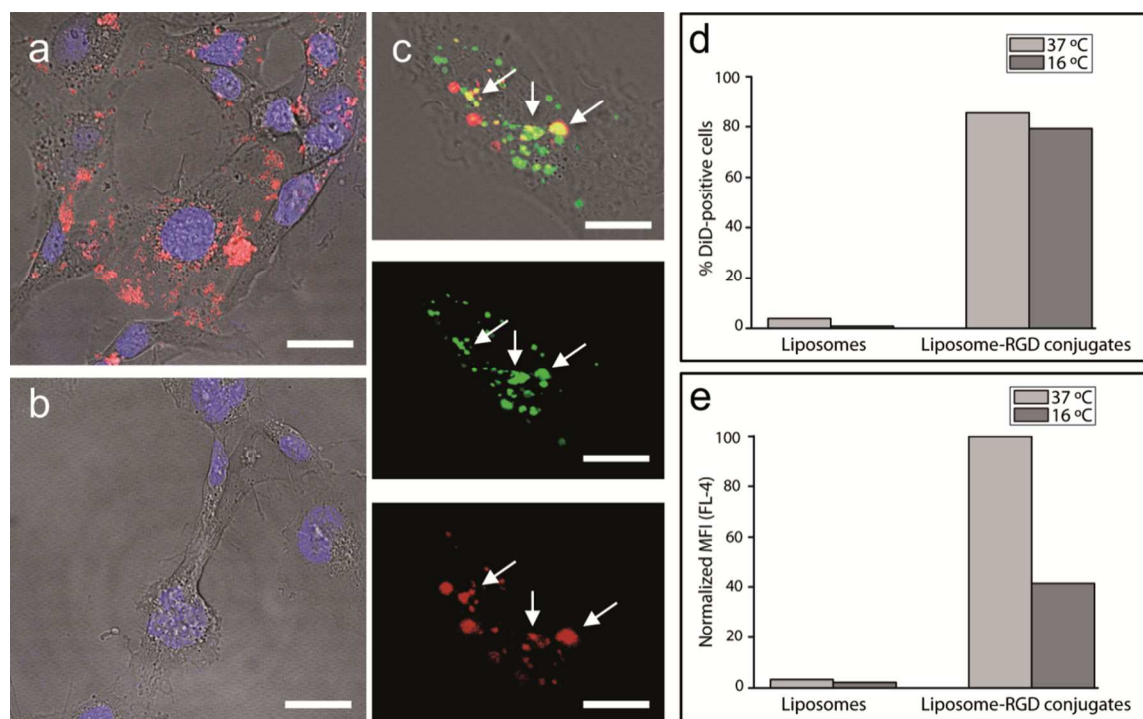


Figure 4. Internalization of nanovesicles on endothelial cells assessed by fluorescence. Confocal images of HMEC-1 cells incubated during 3 hours at 37°C in a 5% of CO₂ atmosphere with a, Liposome-RGD conjugates (red) at 0.3 mg/mL and b, plain Liposomes at 0.3 mg/mL. Cells nuclei were stained with Hoechst 33342 (blue). Scale bars are 10 μm. c, Colocalization of Liposome-RGD conjugates (red) and the lysotracker (green) as observed by confocal microscopy. The upper image shows merging of both signals, where arrows highlight the colocalization of Liposome-RGD conjugates with lysosomal compartments. Independent signals are shown in the lower panels. Scale bars are 10 μm. d, Flow cytometry quantification of the fraction of cells that had bound or internalized plain Liposomes and Liposome-RGD conjugates as the percentage (%) of DiD-positive cells among the total number of cells counted. e, Mean fluorescence intensity (MFI) of DiD in the cells normalized to the maximum fluorescence intensity. Cells were incubated with plain and functionalized Liposomes for 3 hours at 16°C or 37°C.

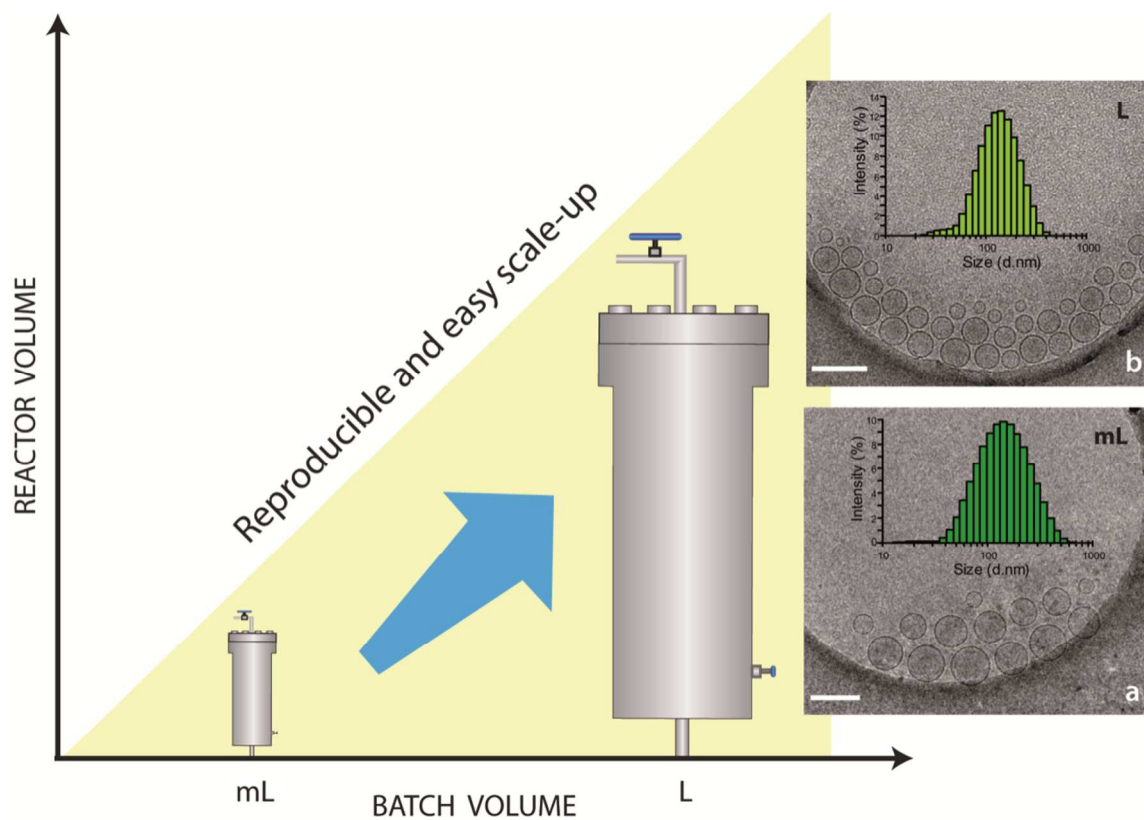


Figure 5. Scale-up of DELOS-SUSP method. BSA protein was integrated into Quatsomes at a concentration of $16 \mu\text{M}$ in water using both a small (7.5 mL) and a large (315 mL) high pressure reactor that produced 27 mL and 1.3 L of an aqueous dispersion of the nanovesicle-bioactive conjugates, respectively. a, Cryo-TEM image and size distribution of BSA protein loaded Quatsomes obtained at small scale. b, Cryo-TEM image and size distribution of the protein loaded Quatsomes obtained at large scale. After scaling-up the nanovesicles maintain similar physicochemical and morphological characteristics. Scale bars are 200 nm.

1
2
3 **TABLES**
4
5
6

7 Table 1. Physicochemical characteristics of the different vesicular formulations obtained by
8
9 DELOS-SUSP method
10

11
12
13

System (Number of batches)	Size		Z potential (mV)
	Mean (nm)	PdI	
Quatsome_PEG ₁₀₀₀ (3)	67 ± 6	0.15 ± 0.07	69 ± 8
Quatsome_PEG ₂₀₀₀ (3)	84 ± 0.5	0.20 ± 0.03	38 ± 1
Liposome_PEG ₁₀₀₀ (3)	138 ± 10	0.4 ± 0.1	13 ± 2
Liposome_PEG ₂₀₀₀ (3)	135 ± 9	0.47 ± 0.04	8 ± 2
Liposome_RGD (4)	144 ± 12	0.19 ± 0.01	31 ± 1
GFP loaded-Liposomes (2)	228 ± 8	0.42 ± 0.02	-1.24 ± 0.06
BSA loaded-Quatsomes (3)	149 ± 12	0.26 ± 0.1	75 ± 7
BSA loaded- Quatsome_PEG ₁₀₀₀ (2)	82 ± 8	0.23 ± 0.01	52 ± 4

14
15
16
17
18
19
20
21
22
23
24
25
26
27
28
29
30
31
32
33
34
35
36
37
38
39
40
41
42
43
44
45
46
47
48
49
50
51
52
53
54
55
56
57
58
59
60

Table 2. Compositions used for the preparation of the different vesicular formulations by DELOS-SUSP method

System	Organic phase	Aqueous phase	Biom/lipid Ratio ($\mu\text{mol}/\text{mmol}$)	Lipidic conc.* (mg/mL)
Quatsome_PEG ₁₀₀₀	Cholesterol (48 mM) + CHOL_PEG ₁₀₀₀ (8 mM)	CTAB (7.8 mM) in water	66	5
Quatsome_PEG ₂₀₀₀	Cholesterol (38 mM) + CHOL_PEG ₂₀₀₀ (6.3 mM)	CTAB (7.8 mM) in water	58	5
Liposome_PEG ₁₀₀₀	Cholesterol (18 mM) + DPPC (27 mM) + CHOL_PEG ₁₀₀₀ (3 mM)	water	64	1.4
Liposome_PEG ₂₀₀₀	Cholesterol (14mM) + DPPC (27 mM) + CHOL_PEG ₂₀₀₀ (2.4 mM)	water	54	1.4
Liposome_RGD	Cholesterol (17 mM) + DPPC (27 mM) + CHOL_PEG _{200-RGD} (2.8 mM)	water	59	1.4
GFP loaded-Liposomes	Cholesterol (26 mM) + DPPC (27 mM)	GFP-H6 (1 μM) in TRIS buffer (pH=7.5)	0.4	1.4
BSA loaded-Quatsomes	Cholesterol (68 mM)	CTAB (7.8 mM) + BSA (16 μM) in water	1	5
BSA loaded-Quatsome_PEG ₁₀₀₀	Cholesterol (48 mM) + Cholesterol_PEG ₁₀₀₀ (8 mM)	CTAB (7.8 mM) + BSA (16 μM) in water	1.2	5

*The lipidic concentration is defined as the total mass of lipids comprising the vesicles divided by the total volume of vesicular suspension.

ASSOCIATED CONTENT

Supporting Information. The Supporting information contains a description of the materials used, the physicochemical characterization of the vesicles, the production of bioactive compounds and the determination of the degree of loading/functionalization in the conjugates. Description of the DELOS-susp method and details on the equipment configurations of the two reactors used is reported. Internalization experiments details and images of the nanovesicles functionalization procedure are shown. Citotoxicity and Hemocompatibility assays are described. Lipid thin-film hydration methodology to produce Liposome-RGD conjugates is reported. Differences in homogeneity of Liposome-RGD conjugates prepared using different methodologies are demonstrated by Cryo-TEM images and DLS measurements. Differences in homogeneity between Liposomes and Liposome-RGD conjugates are demonstrated through SAXS measurements, DLS measurements, and Cryo-TEM images. Dual color EPI-TIRF microscopy images of Liposome-GFP conjugates labelled with DiD are included. This material is available free of charge via the Internet at <http://pubs.acs.org>.

AUTHOR INFORMATION

Corresponding Author

*Tel.: +34 935 801 853. Fax: +34 935 805 729. E-mail: vecianaj@icmab.es, ventosa@icmab.es

Author Contributions

I.C. carried out DELOS-SUSP experiments, the physicochemical characterization of the systems, analyzed the data and wrote the manuscript; E.E. participated in the design and engineering of the small scale reactor and assisted in the manuscript preparation; O.E. carried out the TIRF-EPI

1
2
3 and confocal microscopy measurements, the flow cytometry experiments and the cellular uptake
4 experiments; J.L.C. performed the SDS-page and Western-Blot experiments; M.M. and D.P.
5 synthesized the cholesterol_PEG₂₀₀_RGD molecule and quantified its integration percentage into
6 the liposomes; A.C. participated in the design and engineering of the small scale reactor; E.M.
7 performed the synchrotron SAXS measurements; U.U. and E.V. synthesized the GFP-H6
8 protein; F.A. and M.R. designed the experiments related to Cholesteol:PEG₂₀₀:RGD molecule
9 synthesis and quantification; E.V. and A.V. designed the experiments related to florescent
10 protein manipulation; M.G-P. conceived TIRF-EPI, confocal microscopy, cellular uptake
11 experiments and contributed to the correction of the manuscript ; I.A. designed and performed
12 the cytotoxicity and hemocompatibility assays and S.S.Jr. reviewed the obtained results; N.V
13 conceived the DELOS-SUSP process, provided overall scientific guidance and carried out the
14 final edition of the manuscript; J.V. conceived some experiments, provides scientific guidance
15 and contributed to the correction and final edition of the manuscript.
16
17
18
19
20
21
22
23
24
25
26
27
28
29
30
31
32
33
34
35
36

37 ACKNOWLEDGMENT

38
39
40 We acknowledge financial support from Instituto de Salud Carlos III, through “Acciones
41 CIBER”. The Networking Research Center on Bioengineering, Biomaterials and Nanomedicine
42 (CIBER-BBN) is an initiative funded by the VI National R&D&I Plan 2008-2011,
43 IniciativaIngenio 2010, Consolider Program, CIBER Actions and financed by the Instituto de
44 Salud Carlos III with assistance from the European Regional Development Fund. The authors
45 appreciate the financial support through the project “Development of nanomedicines for
46 enzymatic replacement therapy in Fabry disease”, granted by the *Fundació Marató TV3* and
47 projects POMAS (CTQ2010-019501), granted by DGI (Spain), 2009SGR0516 and
48
49
50
51
52
53
54
55
56
57
58
59
60

2009SGR0108, financed by DGR (Catalunya). The authors wish also to thank the Microscopy Service of UAB, specially Pablo Castro and Ana Tarruella, for the technical support in taking the Cryo-TEM images. AV is recipient of an ICREA Academia (Generalitat de Catalunya) award.

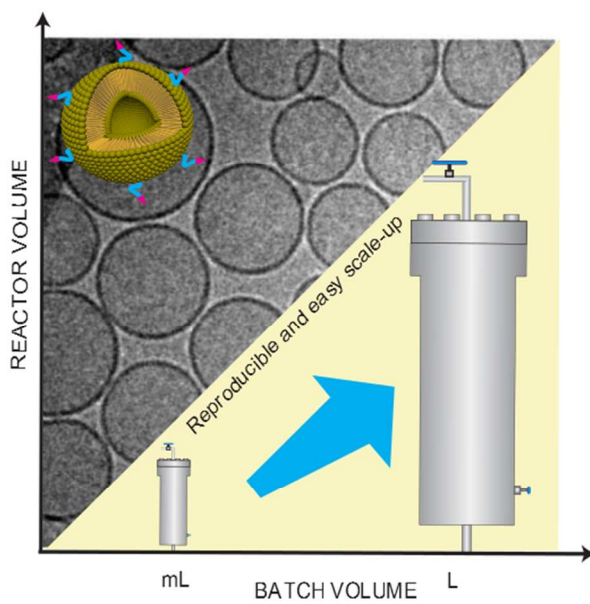
REFERENCES

- (1) Sawant, R. R.; Torchilin, V. P. *Soft Matter* **2010**, *6*, 4026.
- (2) Reflection paper on the data requirements for intravenous liposomal products developed with reference to an innovation liposomal product. European Medicines Agency, http://www.ema.europa.eu/ema/index.jsp?curl=pages/regulation/general/general_content_000564.jsp&mid=WC0b01ac05806403e0
- (3) Peer, D.; Karp, J. M.; Hong, S.; Farokhzad, O. C.; Margalit, R.; Langer, R. *Nature Nanotechnology* **2007**, *2*, 751.
- (4) Duncan, R.; Gaspar, R. *Mol. Pharm.* **2011**, *8*, 2101.
- (5) Farokhzad, O. C.; Langer, R. *ACS Nano* **2009**, *3*, 16.
- (6) Hussain, S.; Pluckthun, A.; Allen, T. M.; Zangemeister-Wittke, U. *Mol. Cancer Ther.* **2007**, *6*, 3019.
- (7) Colletier, J. P.; Chaize, B.; Winterhalter, M.; Fournier, D. *BMC Biotechnology* **2002**, *2*.
- (8) Glavas-Dodov, M.; Fredro-Kumbaradzi, E.; Goracinova, K.; Calis, S.; Simonoska, M.; Hincal, A. A. *Acta Pharmaceutica* **2003**, *53*, 241.
- (9) Szoka, F.; Olson, F.; Heath, T.; Vail, W.; Mayhew, E.; Papahadjopoulos, D. *BBA - Biomembranes* **1980**, *601*, 559.
- (10) Kubo, T.; Sugita, T.; Shimose, S.; Nitta, Y.; Ikuta, Y.; Murakami, T. *International journal of oncology* **2000**, *17*, 309.
- (11) Templeton, N. S.; Lasic, D. D.; Frederik, P. M.; Strey, H. H.; Roberts, D. D.; Pavlakis, G. N. *Nature Biotechnology* **1997**, *15*, 647.
- (12) Yatvin, M. B.; Weinstein, J. N.; Dennis, W. H.; Blumenthal, R. *Science* **1978**, *202*, 1290.
- (13) Mayer, L. D.; Hope, M. J.; Cullis, P. R. *BBA - Biomembranes* **1986**, *858*, 161.
- (14) Olson, F.; Hunt, C. A.; Szoka, F. C.; Vail, W. J.; Papahadjopoulos, D. *Biochimica Et Biophysica Acta* **1979**, *557*, 9.
- (15) Eaton, M. A. W. *Journal of controlled release : official journal of the Controlled Release Society* **2012**, *164*, 370.
- (16) Perrut, M.; Clavier, J. Y. *Ind. Eng. Chem. Res.* **2003**, *42*, 6375.
- (17) Hakuta, Y.; Hayashi, H.; Arai, K. *Curr. Opin. Solid State Mat. Sci.* **2003**, *7*, 341.
- (18) Eckert, C. A.; Knutson, B. L.; Debenedetti, P. G. *Nature* **1996**, *383*, 313.
- (19) Jessop, P. G.; Subramaniam, B. *Chem. Rev.* **2007**, *107*, 2666.
- (20) Cano-Sarabia, M.; Ventosa, N.; Sala, S.; Patiño, C.; Arranz, R.; Veciana, J. *Langmuir* **2008**, *24*, 2433.
- (21) Elizondo, E.; Larsen, J.; Hatzakis, N. S.; Cabrera, I.; Bjornholm, T.; Veciana, J.; Stamou, D.; Ventosa, N. *Journal of the American Chemical Society* **2012**, *134*, 1918.

- 1
2
3 (22) L. Ferrer-Tasies, E. M.-C., M. Cano-Sarabia, M. Aguilera-Arzo, A. Angelova, S.;
4 Lesieur, S. R., J. Faraudo, N. Ventosa, J. Veciana (*10.1021/la4003803*)
5 (23) Cromie, S. R. T.; Ballone, P. *The Journal of chemical physics* **2009**, *131*, 034906.
6 (24) Klibanov, A. L.; Maruyama, K.; Torchilin, V. P.; Huang, L. *FEBS Lett.* **1990**,
7 268, 235.
8 (25) Moghimi, S. M.; Hunter, A. C.; Murray, J. C. *Pharmacological Reviews* **2001**, *53*,
9 283.
10 (26) Dubey, P. K.; Mishra, V.; Jain, S.; Mahor, S.; Vyas, S. P. *Journal of drug*
11 *targeting* **2004**, *12*, 257.
12 (27) Temming, K.; Schiffelers, R. M.; Molema, G.; Kok, R. J. *Drug resistance updates*
13 *: reviews and commentaries in antimicrobial and anticancer chemotherapy* **2005**, *8*, 381.
14 (28) Schiffelers, R. M.; Koning, G. A.; Ten Hagen, T. L. M.; Fens, M. H. A. M.;
15 Schraa, A. J.; Janssen, A. P. C. A.; Kok, R. J.; Molema, G.; Storm, G. *Journal of Controlled*
16 *Release* **2003**, *91*, 115.
17 (29) Xu, Y. L.; Swerlick, R. A.; Sepp, N.; Bosse, D.; Ades, E. W.; Lawley, T. J.
18 *Journal of Investigative Dermatology* **1994**, *102*, 833.
19 (30) Ventosa-Rull, N. C., I.; Elizondo, E.; Veciana, J.; Sala, S.; Melgarejo, M.;
20 Royo, M.; Albericio, F.; Pulido, D. *Spanish Patent Appl. P201231020* **2012**.
21 (31) Pisal, D. S.; Kosloski, M. P.; Balu-Iyer, S. V. *Journal of pharmaceutical sciences*
22 **2010**, *99*, 2557.
23 (32) Hubbell, J. A. *Science* **2003**, *300*, 595.
24 (33) Luisa Corvo, M.; Jorge, J. C. S.; Van't Hof, R.; Cruz, M. E. M.; Crommelin, D. J.
25 A.; Storm, G. *Biochimica et Biophysica Acta - Biomembranes* **2002**, *1564*, 227.
26 (34) Kisel, M. A.; Kulik, L. N.; Tsybovsky, I. S.; Vlasov, A. P.; Vorob'yov, M. S.;
27 Kholodova, E. A.; Zabarovskaya, Z. V. *International Journal of Pharmaceutics* **2001**, *216*, 105.
28 (35) Xu, X.; Costa, A.; Burgess, D. J. *Pharmaceutical research* **2012**, *29*, 1919.
29 (36) Chalfie, M.; Tu, Y.; Euskirchen, G.; Ward, W. W.; Prasher, D. C. *Science* **1994**,
30 263, 802.
31 (37) Nasevicius, A.; Ekker, S. C. *Nature Genetics* **2000**, *26*, 216.
32 (38) Uskova, M. A.; Borst, J. W.; Hink, M. A.; Van Hoek, A.; Schots, A.; Klyachko,
33 N. L.; Visser, A. J. W. G. *Biophysical Chemistry* **2000**, *87*, 73.
34 (39) Holgado, M. A.; Cozar-Bernal, M. J.; Salas, S.; Arias, J. L.; Alvarez-Fuentes, J.;
35 Fernandez-Arevalo, M. *Int J Pharm* **2009**, *380*, 147.
36 (40) Worsdorfer, B.; Pianowski, Z.; Hilvert, D. *Journal of the American Chemical*
37 *Society* **2012**, *134*, 909.
38 (41) Yokouchi, Y.; Tsunoda, T.; Imura, T.; Yamauchi, H.; Yokoyama, S.; Sakai, H.;
39 Abe, M. *Colloids and Surfaces B: Biointerfaces* **2001**, *20*, 95.
40 (42) Maulik, S.; Dutta, P.; Chattoraj, D. K.; Moulik, S. P. *Colloids and Surfaces B:*
41 *Biointerfaces* **1998**, *11*, 1.
42 (43) Dai, C.; Wang, B.; Zhao, H.; Li, B.; Wang, J. *Colloids and surfaces. B,*
43 *Biointerfaces* **2006**, *47*, 205.
44 (44) Ventosa-Rull, L. C., I.; Veciana, J.; Santana, H.; Martinez, E., Berlanga, J. A.
45 *Cuban Patent Appl. CU2012-0112* **2012**.
46 (45) Martins, S.; Sarmiento, B.; Ferreira, D. C.; Souto, E. B. *International journal of*
47 *nanomedicine* **2007**, *2*, 595.
48
49
50
51
52
53
54
55
56
57
58
59
60

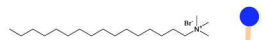
1
2
3 (46) Lesoin, L.; Boutin, O.; Crampon, C.; Badens, E. *Colloids and Surfaces A: Physicochemical and Engineering Aspects* **2011**, 377, 1.
4
5
6
7
8
9
10
11
12
13
14

15 **TOC graphic**

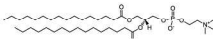


DELOS-SUSP**Synthesis of nanovesicles**

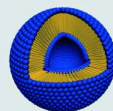
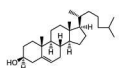
CTAB



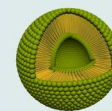
DPPC



CHOLESTEROL



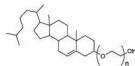
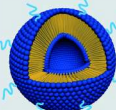
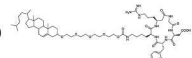
Quatsomes



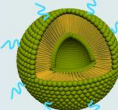
Liposomes

Functionalization with stabilizing/targeting moieties

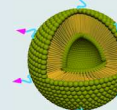
CHOL_PEGs

CHOL_PEG₂₀₀_RGD

Pegylation of Quatsomes



Pegylation of Liposomes



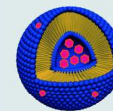
Liposomes targeted with RGD peptide

Integration of hydrophilic proteins

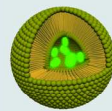
Green Fluorescent Protein (GFP)



Bovine Serum Albumin (BSA)



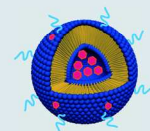
BSA@Quatsomes



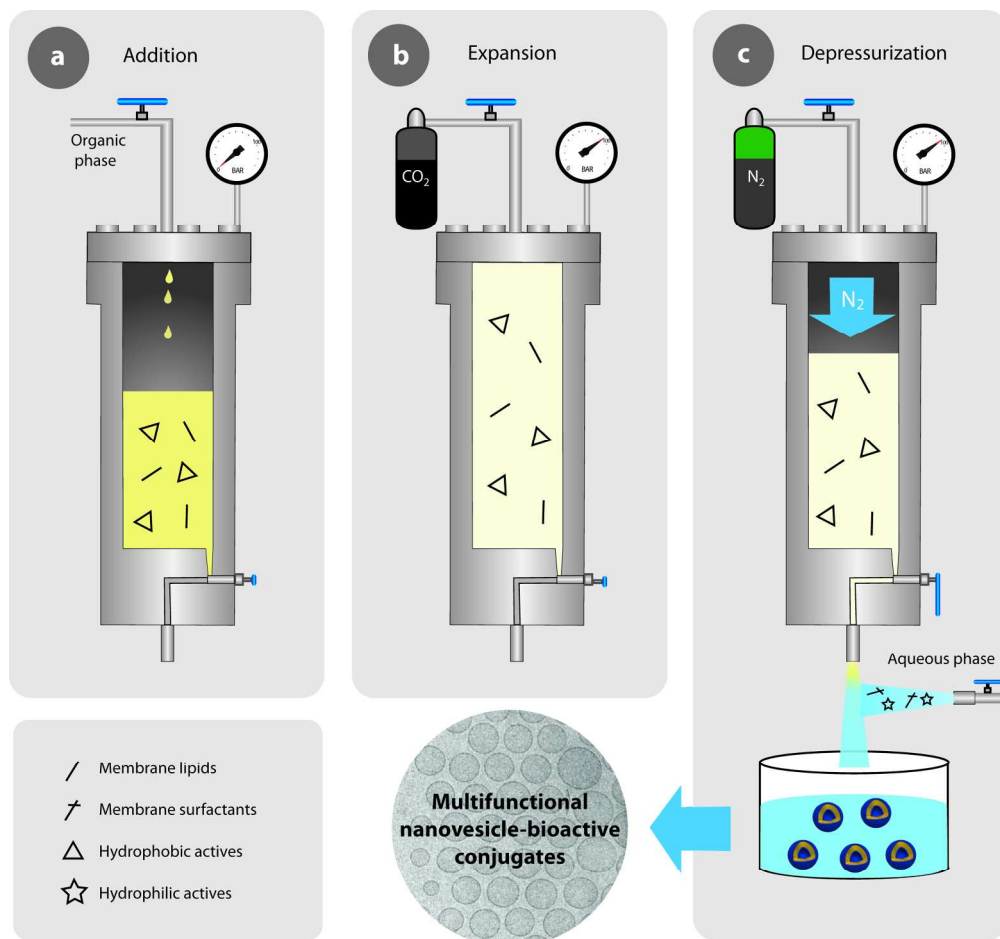
GFP@Liposomes

Simultaneous functionalization and protein integration

Bovine Serum Albumin (BSA)

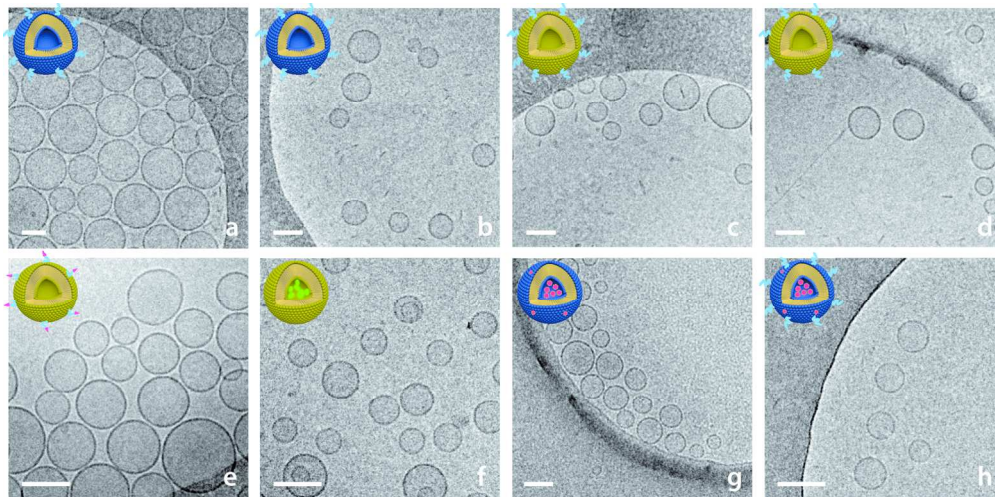
CHOL_PEG₁₀₀₀BSA@Quatosome_PEG₁₀₀₀

207x246mm (300 x 300 DPI)

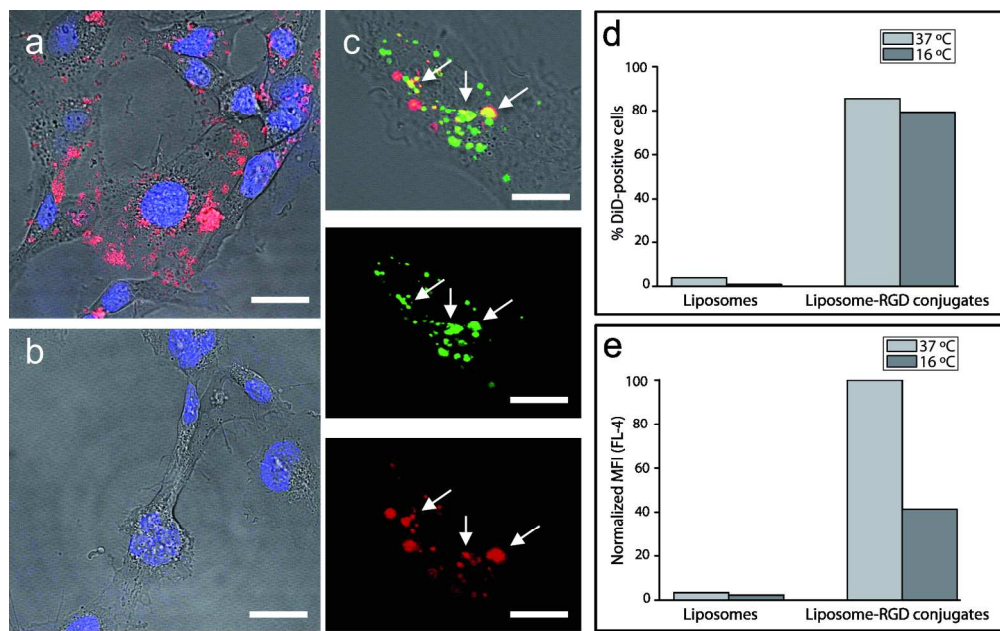


186x180mm (300 x 300 DPI)

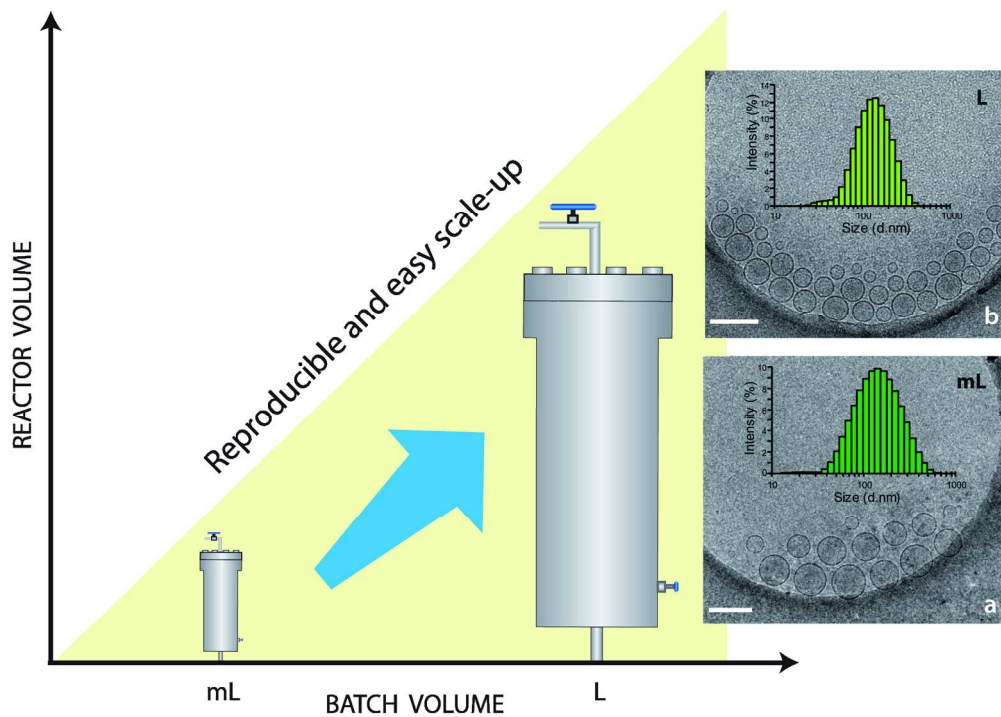
1
2
3
4
5
6
7
8
9
10
11
12
13
14
15
16
17
18
19
20
21
22
23
24
25
26
27
28
29
30
31
32
33
34
35
36
37
38
39
40
41
42
43
44
45
46
47
48
49
50
51
52
53
54
55
56
57
58
59
60



167x82mm (300 x 300 DPI)



170x106mm (300 x 300 DPI)



161x114mm (300 x 300 DPI)

1
2
3
4
5
6
7
8
9
10
11
12
13
14
15
16
17
18
19
20
21
22
23
24
25
26
27
28
29
30
31
32
33
34
35
36
37
38
39
40
41
42
43
44
45
46
47
48
49
50
51
52
53
54
55
56
57
58
59
60